

## Heaping and secondary flows in sheared granular materials

Ralf Stannarius<sup>1,\*</sup>, David Fischer<sup>1,\*\*</sup>, and Tamás Börzsönyi<sup>2,\*\*\*</sup>

<sup>1</sup>*Institute of Experimental Physics, Otto von Guericke University, Universitätsplatz 2, 39106 Magdeburg, Germany*

<sup>2</sup>*Institute for Solid State Physics and Optics, Wigner Research Center for Physics, Hungarian Academy of Sciences, P.O. Box 49, H-1525 Budapest, Hungary*

**Abstract.** Split-bottom cylindrical containers are well established devices in experiments where granular materials are continuously sheared. They are characterized by localized broad shear bands. In such shear experiments, shape-anisotropic grains develop a secondary flow profile in the radial direction. A macroscopically observable consequence is the formation of a heap in the center of the container. This effect is found for all investigated types of prolate and oblate grains, but it is completely absent for spherical particles. There are qualitative differences in the behavior of short (moderate aspect ratio  $< 8$ ) and long grains. The fill height of the granulate in the container considerably affects the time scale for heap formation, while the height of the heap is less dramatically influenced. Under reversal of the shear direction, the heap collapses within a few rotations, before the secondary flow in the reverse direction establishes a new heap.

### 1 Introduction

Granular flows are present in countless processes encountered in geology, transport of materials like sand, coal or ores, and agricultural products. It also affects our everyday life in the kitchen or offices whenever we stir or shake grainy matter or pour it out of a container. However, while flow in Newtonian fluids has been well understood for centuries, and even many non-Newtonian flow phenomena are well characterized in liquids, granular flows have still preserved their mysteries to a great deal. Different aspects of granular dynamics were discussed in books and review articles (e.g. [1–5]). Peculiarities of shape-anisotropic granular matter have been reviewed recently [6], with focus on specific packing problems, shear flow, alignment and orientational order.

Recently, the phenomenon of secondary flow has attracted the interest of researchers in different fields of granular matter physics (e.g. [7–20]). One prominent example where secondary flow effects manifest themselves is the heaping of elongated grains under shear in a cylindrical geometry [19]. The formation of these structures as well as the dynamics of the secondary flow and its dependence on particle shapes and geometrical parameters of the setup have been studied in detail by Fischer et al. [20]. Wortel et al. [19] gave the following description of the phenomenon: Elongated grains form a heap in the center, which reaches a saturation height after a certain number of rotations. When the sense of rotation is reversed, the heap first collapses but thereafter reappears at a comparable time scale as from the disordered initial state. The

fill level of the container has considerable influence on the phenomenon. The optimal fill height for heap formation is when the granulate at the surface above the revolving disk rotates with approximately half the disk velocity. A convective flow was detected by means of X-ray CT. Fischer et al. [20] showed that heaping is also found in oblate material. They demonstrated the influence of the fill height on the time scales of heap formation and presented the results with numerical simulations. We compare the experimental data for different rotationally symmetric grain shapes (cylindrical and ellipsoidal) and discuss the dependence of the secondary flow on these parameters and the geometry of the experiment.

### 2 Experimental method

Cylindrical containers with split-bottom have been introduced [4, 21, 22] to study granular materials under continuous shear. The central part of the bottom can be rotated with respect to the outer container, the granulate develops a broad shear zone [21]. Observation and analysis of the particle arrangements and dynamics can be performed optically at the granular surface [19–23], or in an index-matching fluid with a Laser sheet [24], destructively by excavation [25–27], or non-invasively by X-ray CT [26, 27, 30, 31] and Magnetic Resonance Imaging [28, 29].

Two geometries are explored in our investigation, the first one shown in Figure 1a is the conventional split-bottom experiment. All quantitative results presented here are obtained in this geometry. The second one shown in Figure 1b includes a vertical cylinder above the center of the rotating disk, much smaller than the disk size. Some qualitative results with this geometry are described below.

\* e-mail: ralf.stannarius@ovgu.de

\*\* e-mail: david.fischer@ovgu.de

\*\*\* e-mail: borzsonyi.tamas@wigner.mta.hu

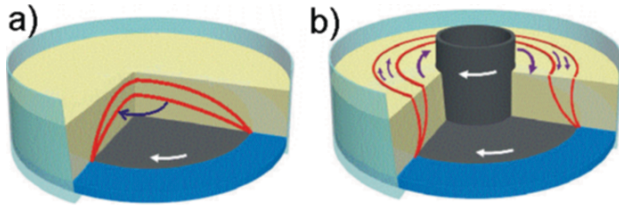


**Figure 1.** Sketch of the experimental setup and the location of the shear zones. a) In the first geometry of a simple rotating bottom plate, the shear zone can form a closed dome when the fill level of the container is low, or it forms an open ring as in b) when the fill level is sufficiently high. In the geometry b) with the inner cylinder, the shear zone has always an open ring shape.

The central part can be rotated by a motor at constant rates up to about 27 rpm, the outer part of the container remains fixed. The investigated materials and their properties are listed in Table 1.

**Table 1.** Lengths  $\ell$ , diameters  $d$  and aspect ratios  $Q$  of the investigated grain types. The images reflect realistic size ratios.

	material	$\ell$ [mm]	$d$ [mm]	$Q$
	plastic cyl.	24	2	12
	wooden peg	25	5	5
	glass cyl.	6.6	1.9	3.5
	airsoft ball	-	6	1
	pea	-	7	$\approx 1$
	lentil	2.5	7	0.36

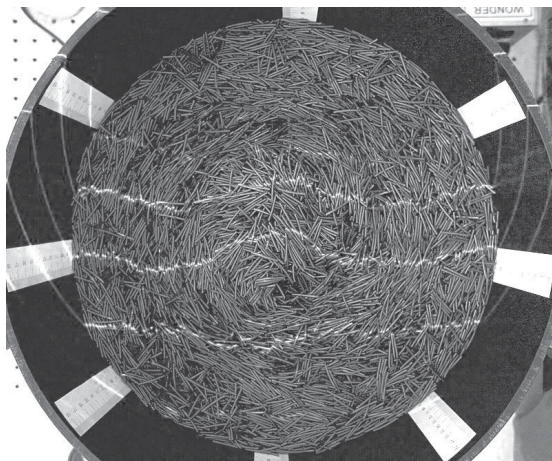


**Figure 2.** Top view of the experiment with elongated cylinders ( $Q = 12$ ) after the heap is fully developed. The distortion of the Laser reflection lines indicates the height profile in different regions. Here, multiple Laser lines visualize the asymmetry of the heap.

The top of the granular surface is illuminated with a He-Ne Laser sheet at an incident angle of  $45^\circ$ . A camera mounted vertically above the container allows us to record the horizontal displacement of the Laser reflec-

tion. From this shift, the radial profile of the emerging heap is calculated [20]. With an array of Laser lines (Figure 2), accomplished by a combination of a line Laser and a diffraction lattice, multiple scans of the granular surface can be recorded simultaneously during the shear experiment. This allows us to obtain more details when the heap profile is not axially symmetric.

### 3 Results

First, we discuss experiments in the geometry of Figure 1a: The formation of the heap extracted from the optical analysis of the surface profile is shown in Figure 3 for particles of different aspect ratios. We define the heap height  $h_{\max}$  as the highest elevation of the granular surface in the container, relative to the initial, uniform fill level. The parameters for the graph of the  $Q = 3.5$  glass rods are fill height  $h_0 = 75$  mm, rotation rate of the bottom disk  $\omega = 4.7$  rpm, for the  $Q = 5$  pegs  $h_0 = 75$  mm,  $\omega = 3$  rpm, for the lentils  $h_0 = 70$  mm,  $\omega = 10$  rpm, and for the long  $Q = 12$  plastic rods  $h_0 = 90$  mm,  $\omega = 5$  rpm. Heaping is observed for all investigated anisometric grain types, there is no clear trend in the final heap height vs. particle aspect ratio. For the perfectly spherical airsoft balls,  $h_0 = 75$  mm, for the peas  $h_0 = 80$  mm. Rotation rates of the bottom disk are 5 rpm in both cases. The fluctuations of the surface are less than one particle diameter in both cases.

In all experiments with anisometric grains except the long ( $Q = 12$ ) rods, the peak appears directly above the central axis of the bottom disk, and the heap is axially symmetric (peculiarities of the  $Q = 12$  material will be discussed in the next paragraph). For all other rods, the characteristic times of heap formation are comparable. The peak shape after the initial transient is stationary (see also Figure 5 below). This confirms earlier observations with different grain types (see Figures 6, 7, 9, 11 in Ref. [20]).

The long rods with aspect ratio  $Q = 12$  behave qualitatively different. The heap forms above the rotating bottom disk (i. e. within the outer diameter of the disk), but not necessarily axially symmetric with respect to the rotation center. This asymmetry is evident in the profiles of the multiple Laser lines in Figure 2. A typical temporal evolution of the surface profile along a central cross section, illuminated by the single Laser sheet, is shown in the space-time plot of Figure 4: The off-axis heap rotates with the precession of the granulate, and moreover it performs slow structure changes (slow in the sense that it requires several dozen rotations of the disk for relevant shape changes of the heap). The heap shape is not stationary neither in the laboratory frame nor in the local co-rotating frame of the granular surface. Not only the position of the heap changes, but also the heap height fluctuates considerably. The short-period shifts of the peak in Figure 4 reflect the precession of the off-axis heap around the center. It is accompanied by a modulation of the absolute height with a period of about 15 revolutions of the bottom disk. This is also reflected in the fluctuations in Figure 3.

The contrast to the behavior of the shorter grains is evident in the comparison with Figure 5, top. There, the

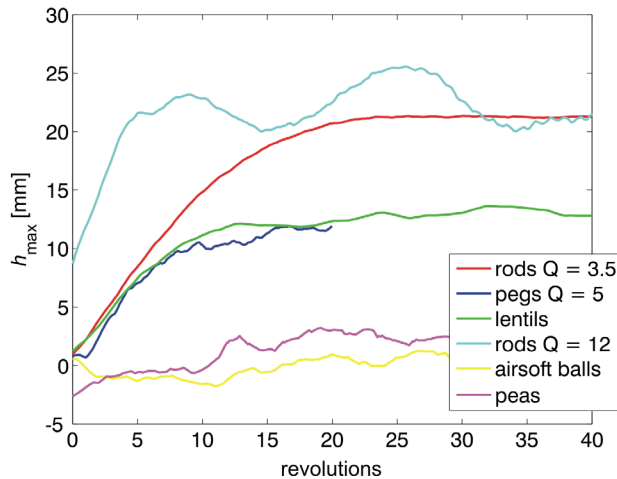


**Figure 3.** Evolution of the heap from the initial flat surface. The heap height  $h_{\max}$  is defined as the highest point of the granular bed relative to the initial fill level. All measurements are performed with the optimum fill heights of the container (upper surface above the rotating disk rotates with approximately half the rate of the disk). The  $Q = 12$  cylinders show large long-term fluctuations not only of the position of the peak, but also of its magnitude.

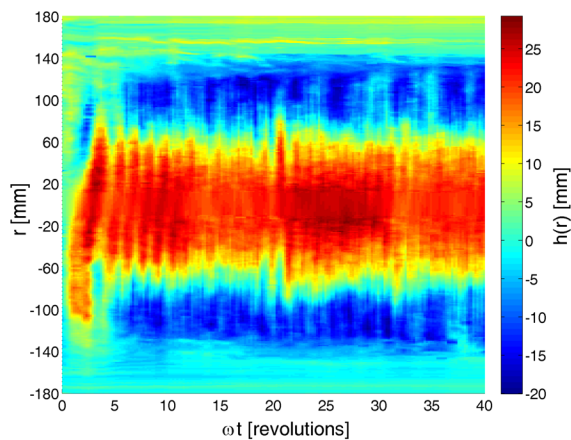


**Figure 4.** Temporal evolution of the cross section profile for plastic rods of  $Q = 12$ . It is evident that the heap is not located directly above the rotation axis. It rotates with the precession frequency of the granular surface but also undergoes slow structure reorganizations on the time scale of dozens of rotations.  $h_0 = 90$  mm,  $\omega = 5$  rpm

heap is central and symmetric and it does not noticeably fluctuate in shape. The bottom image of Figure 5 shows collapse and recovery of the peak when the rotation direction of the bottom disk is reversed. Peak formation is reproducible and independent of the shear direction. After each reversal, the peak re-appears with the same profile and same height, in sharp contrast to the  $Q = 12$  rods where the positions and heights of the heap are not exactly reproducible.

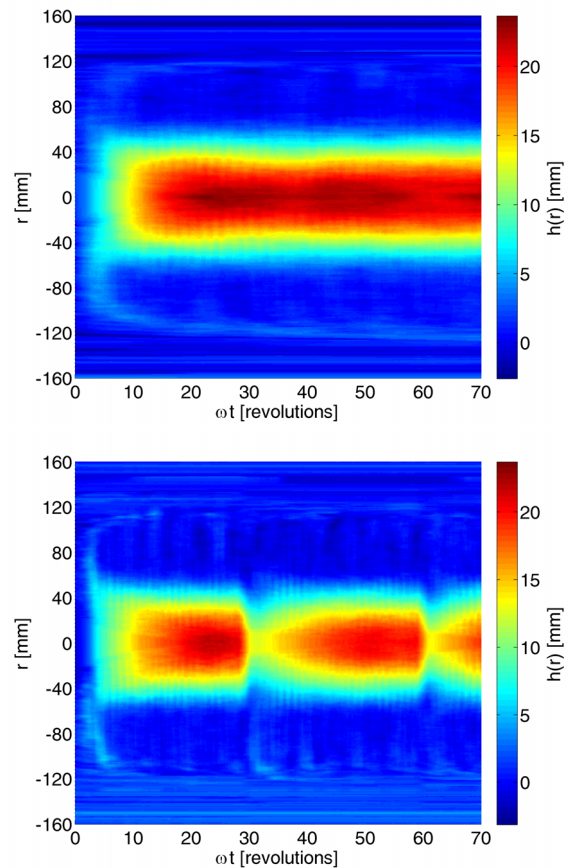


**Figure 5.** Evolution of the heap profile of  $Q = 3.5$  glass rods under constant shear (top) and during successive reversal of the shear direction every 30 revolutions (bottom). The heap collapses almost instantly after shear reversal, but thereafter recovers with a rate comparable to the initial growth rate. After the heap has formed, it remains stationary. This is in sharp contrast to the dynamics of the long rods shown in Figure 4.

Finally, we describe qualitatively the experiments with a central vertical cylinder (Figure 1b). In this modified geometry, the heap formation is suppressed. If the cylinder has a large diameter (e.g. 16 cm cylinder above a 39 cm bottom disk), then one finds only a shallow wall around the cylinder, no heap, and the surface profile slightly decreases from that wall to the cylinder surface (Figs. 4, 11 in Ref. [31]). But even with a narrow cylinder, with a diameter of the order of a few grains, we find only a circular wall around it, with a slight depletion towards the cylinder surface. Obviously, the vertical flow in the convection vortex is inhibited at the cylinder surface, and thus the heaping process is much less effective there. The convection still takes place, but the roll ends inwards at some distance from the vertical cylinder wall. This distinguishes the observed heaping in anisometric granular matter from the at first glance very similar phenomenon of rod climbing (Weissenberg effect [33]) in some complex liquids. There, the rotation of a rod inside the liquid leads to the climbing of the liquid upwards at the rod surface.

## 4 Discussion and Summary

It has been demonstrated [20] that heaping in cylindrical split-bottom containers is characteristic for both prolate and oblate particles, while for all spherical or near-spherical grains the surface remains flat, without heaping. These experiments have been extended to high aspect ratios. The results give evidence that the heaping phenomenon changes qualitatively for the material with aspect ratio  $Q = 12$ , in contrast to the materials with lower aspect ratios, no stationary central heap is formed. Instead, we find fluctuating off-axis heaps. We note that this cannot be the consequence of the large ratio of particle length and bottom disk size, since this ratio is even larger for the  $Q = 5$  pegs, which nevertheless form a stationary central heap. It is rather an indication that the dynamic behavior of such materials cannot simply be extrapolated from the dynamics of less anisometric grains. At large aspect ratios, qualitatively new features have to be taken into account. This agrees with studies of hopper discharge of the same grain types [32].

Comparison of the heap formation process in the geometries of Figure 1a,b emphasizes the importance of details of the shear geometry. On first glance, the observed heaping reminds one of the Weissenberg (rod-climbing) effect in complex fluids. However, the latter effect is even qualitatively different from the heaping observed here. A completely different physical origin has to be sought, irrespective of some striking phenomenological similarities. The effect described here should be studied in detail in other geometries, in order to reveal whether the heaping phenomenon is restricted to the cylindrical split-bottom container, or whether it is also present in a linear shear cell (two L-shaped sliders). Such experiments will help to clarify the nature of the convection, which is still not understood satisfactorily.

## Acknowledgements

Financial support from the DAAD/MÖB researcher exchange program (Grants No. 57141022 and 64975), from DFG (Grant STA 425/38), and from OTKA (Grant No. OTKA NN 107737) is acknowledged. The authors thank Torsten Trittel for technical assistance and helpful advice.

## References

- [1] H. M. Jaeger, S. R. Nagel, and R. P. Behringer, *Rev. Mod. Phys.* **68** 1259-1273 (1996)
- [2] J. Duran, *Sands, Powders, and Grains*, (Springer New York, 2000)
- [3] I. S. Aranson and L. S. Tsimring, *Rev. Mod. Phys.* **78** 641-692 (2006)
- [4] J. A. Dijksman and M. van Hecke, *Soft Matter* **6** 2901 - 2907 (2010)
- [5] M.C. Marchetti et al., *Rev. Mod. Phys.* **85** 1143-1189 (2013)
- [6] T. Börzsönyi R. and Stannarius, *Soft Matter* **9** 7401 (2013)
- [7] J. B. Knight, H. M. Jaeger, and S. R. Nagel, *Phys. Rev. Lett.* **70** 3728 (1993)
- [8] R. Khosropour, J. Zirinsky, H. K. Pak, and R. P. Behringer, *Phys. Rev. E* **56** 4467 (1997)
- [9] S. Laín, M. Sommerfeld, and B. Quintero, *Brazil. J. Chem. Eng.* **26** 583 (2009)
- [10] V. Vidyapati et al., *Powder Techn.* **220** 7-14 (2012)
- [11] M. Alletto and M. Breuer, *Int. J. Multiphase Flow* **55** 80-98 (2013)
- [12] M. Harrington, J. H. Weijs, and W. Losert, *Phys. Rev. Lett.* **111** 078001 (2013)
- [13] N. Murdoch et al., *Phys. Rev. Lett.* **110** 018307 (2013)
- [14] J. Havlica, K. Jiroukova, T. Travnickova, M. Kohout, *Powder Techn.* **280** 180-190 (2015)
- [15] K. P. Krishnaraj and P. R. Nott, *Nature Comm.* **7** 10630 (2016)
- [16] T. M. Yamada and H. Katsuragi, *Planetary and Space Sci.* **100** 79-86 (2014)
- [17] F. Zhang, Li Wang, C. Liu, P. Wu, and S. Zhan, *Phys. Letters A* **378** 1303-1308 (2014)
- [18] T. M. Yamada, K. Ando, T. Morota, and H. Katsuragi, *ICARUS* **272** 165-177 (2016)
- [19] G. Wortel, T. Börzsönyi, E. Somfai, S. Wegner, B. Szabó, R. Stannarius, and M. van Hecke, *Soft Matter* **11** 2570-2576 (2015)
- [20] D. Fischer, T. Börzsönyi, D. Nasato, T. Pöschel, and R. Stannarius, *New J. Phys.*, **18**, 113006 (2016)
- [21] D. Fenistein and M. van Hecke, *Nature* **425** 256 (2003)
- [22] D. Fenistein, J. W. van de Meent, and M. van Hecke, *Phys. Rev. Lett.* **92** 094301 (2004)
- [23] R. Moosavi et al., *Phys. Rev. Lett.* **111** 148301 (2013)
- [24] S. Slotterback, M. Mailman, K. Ronaszegi, M. van Hecke, M. Girvan, and W. Losert, *Phys. Rev. E* **85** 021309 (2012)
- [25] D. Fenistein, J.-W. van de Meent, and M. van Hecke, *Phys. Rev. Lett.* **96** 118001 (2006)
- [26] T. Börzsönyi et al., *Phys. Rev. Lett.* **108** 228302 (2012)
- [27] T. Börzsönyi et al., *Phys. Rev. E* **86** 051304 (2012)
- [28] X. Cheng et al., *Phys. Rev. Lett.* **96** 038001 (2006)
- [29] K. Sakaie, D. Fenistein, T. J. Carroll, M. van Hecke, and P. Umbanhowar, *Europhys. Lett.* **84** 38001 (2008), *Europhys. Lett.* **84** 49902 (2008)
- [30] S. Wegner, T. Börzsönyi, T. Bien, G. Rose, and R. Stannarius, *Soft Matter* **8** 10950-10958 (2012)
- [31] S. Wegner et al., *Soft Matter* **10** 5157-5167 (2014)
- [32] A. Ashour, S. Wegner, T. Trittel, T. Börzsönyi, and R. Stannarius, *Soft Matter* **13** 402 (2017)
- [33] K. Weissenberg, *Nature* **159** 310-311 (1947).